AIAA JOURNAL
Vol. 36, No. 1, January 1998

Determination of Buckling Speed for Rotating Orthotropic Disk Restrained at Outer Edge

Naki Tutuncu* and Ali Durdu†
Çukurova University, 01330 Adana, Turkey

The critical angular speed of rotating polar orthotropic circular plates whose outer boundary is constrained from deforming radially is obtained as a function of ply orientation angle. Because the expressions obtained for radial compressive stresses formed due to centrifugal forces were complicated, attaining a closed-form solution of the governing differential equation was not possible. Galerkin formulation of the finite element method has been resorted to, and the results are presented for a full plate and for a plate fixed at its center to a rigid shaft. Increasing the angle of ply orientation up to a certain value decreased the critical speed. In the case of a concentric shaft, increasing the shaft radius increased the critical speed, contributing to the stability of the plate.

Nomenclature

A_{ij}	= in-plane laminate stiffness matrix, $i, j = 1, 2, 6$
a	= radius of rigid shaft
D_{ij}	= in-plane laminate flexural stiffness matrix, $i, j = 1, 2, 6$
E_i	= Young's modulus in the i direction, $i = x, y$
h	= uniform plate thickness
$[K]$	= flexural stiffness matrix of the whole structure
$[K^e]$	= flexural stiffness matrix of a finite element
M_i	= bending moment components, $i = r, \theta$
$[M]$	= geometric stiffness matrix of the whole structure
$[M^e]$	= geometric stiffness matrix of a finite element
N_i	= stress components, $i = r, \theta, r\theta$
Q_{ij}	= transformed in-plane stiffness matrix of the kth lamina
R	= plate radius
r, θ, z	= cylindrical coordinates
t	= ply thickness
u, v, w	= radial, circumferential, and out-of-plane displacement, respectively
z_k	= algebraic distances of bottom and top of kth ply from the midplane of a laminate
$\varepsilon_r, \varepsilon_\theta, \gamma_{r\theta}$	= in-plane strain components in cylindrical coordinates
κ_i	= curvature, $i = r, \theta, r\theta$
λ^2	= ratio of circumferential stiffness to radial stiffness
$\nu_{r\theta}$	= major Poisson's ratio
ρ	= mass per unit area
Φ	= ply orientation angle
ω	= angular speed of rotating plate

I. Introduction

RECENT advances in engineering technologies have made it necessary to design new structural components that either are required to resist severe environmental conditions or are flexible enough in their configuration to yield desired properties in desired directions. Where the conventional isotropic materials remain short of fulfilling these requirements, composite materials that possess anisotropic properties are brought into use.

Composite structural elements such as thin circular plates may find many applications in aerospace industries that require strong, stiff, and lightweight components. The present study is concerned with the stability analysis of rotating composite disks that display polar orthotropic material characteristics. Polar orthotropy is achieved when the polar coordinate axes are also the axes of material symmetry. Various models to determine the stress distribution due to centrifugal forces in rotating disks are abundantly available in the literature. The authors of Refs. 1–5 used an elasticity approach to determine the stresses in orthotropic, single-ply, rotating circular plates with the outer boundary free of any constraints. Bert[6] and Bert and Niedenfuhr[7] used a laminated plate theory on layered plates with extension-bending coupling and with stress-free boundaries by which approximate solutions were obtained. The effect of anisotropy on stresses in rotating disks placed in a stiff casing was studied by Tutuncu,[8] and it was shown that compressive stresses began to occur near the outer boundary. If the rotational speed reaches a critical value, these stresses will cause local buckling. Research papers pertaining to the stability analysis of rotating plates are scarce. A notable work on the subject is Ref. 9, in which the critical rotational speed of an isotropic plate is determined in terms of transcendental functions. The works of Haughton and Ogden[10,11] may be cited among the bifurcation studies of rotating circular cylindrical members. The purpose of the present paper is to assess the critical speed of a rotating orthotropic plate. Polar orthotropy is attained in cross-ply symmetric laminates (all plies are oriented at 0 and 90 deg with respect to the radial coordinate axis) and in balanced laminates with many plies (for each ply oriented at $+\Phi$, there exists a ply oriented at $-\Phi$). For a given laminate thickness, increasing the number of plies n in a balanced laminate decreases the in-plane bending-stretching coupling terms by the factor n. Isotropic plates with stiffeners properly placed in radial and circumferential directions may also be considered to have overall orthotropic properties.

The circular rotating plate either is a full plate or is fixed to a shaft of radius a. In both cases the outer boundary is constrained from deforming radially. Because of additional material complexities involved regarding composites, it becomes quite difficult to obtain closed-form solutions, forcing the researcher to employ numerical procedures. Upon the derivation of the governing differential equation of elastic stability, the finite element method using Galerkin formulation has been chosen to determine the critical speed of rotation. The classical laminated plate theory has been used throughout the analysis. There may be critical speeds associated with a number of deformation modes. The present paper considers only the critical speed for the case of transverse bending. Material nonlinearities are not considered. For isotropic plates, the critical speed associated with in-plane deformation would be considerably larger if material nonlinearities are ignored,[12] but this may not necessarily be so for anisotropic plates.

II. Radial Stresses in Rotating Disks

Consider a circular plate of radius R and uniform thickness h that is rotating with angular speed ω about an axis perpendicular to its

Received July 27, 1996; revision received July 30, 1997; accepted for publication Aug. 30, 1997.

*Assistant Professor of Mechanics, Department of Mechanical Engineering.

†Graduate Student, Department of Mechanical Engineering.

plane. Assuming steady rotation, symmetric deformation, and no bending, displacement fields take the following form:

$$u = u(r), \qquad v = v(\theta) = 0, \qquad w = w(r) = 0 \tag{1}$$

Because of axisymmetry of the problem, all of the stress and strain components are independent of the θ coordinate. The in-plane strain components are

$$\varepsilon_r = \frac{\mathrm{d}u}{\mathrm{d}r}, \qquad \varepsilon_\theta = \frac{u}{r}, \qquad \gamma_{r\theta} = 0 \tag{2}$$

To obtain the governing equations of displacement, the stresses and displacements must be related through Hooke's law. Noting that the problem is a plane-stress problem and in specially orthotropic plates the in-plane and bending equations are uncoupled, the stress-strain relations take the following form:

$$\begin{Bmatrix} N_r \\ N_\theta \\ N_{r\theta} \end{Bmatrix} = \begin{bmatrix} A_{11} & A_{12} & 0 \\ A_{21} & A_{22} & 0 \\ 0 & 0 & A_{66} \end{bmatrix} \begin{Bmatrix} \varepsilon_r \\ \varepsilon_\theta \\ 0 \end{Bmatrix} \tag{3}$$

where N_r and N_θ are, respectively, the stresses in the r and θ directions. Subscripts 1 and 2 refer, respectively, to the r and θ directions, and the stiffness terms are defined in the customary manner as[13]

$$[A] = \sum_{k=1}^{n} \left[Q^{(k)}\right]\{Z_{k+1} - Z_k\}$$

Substituting Eq. (2) into Eq. (3) and thus obtaining expressions for N_r and N_θ in terms of stiffness terms and radial displacement, the equilibrium equations can now be used to derive the governing equation of radial displacement. The only nontrivial equilibrium equation is in the radial direction[14]:

$$\frac{1}{r}\left[\frac{\mathrm{d}}{\mathrm{d}r}(rN_r) - N_\theta\right] + \rho\omega^2 r = 0 \tag{4}$$

Note that $\rho\omega^2 r$ is the externally applied centrifugal force. Substitution of expression for N_r and N_θ in terms of stiffness terms and radial displacement yields the following Cauchy equation for u:

$$r^2 u'' + ru' - (A_{22}/A_{11})u = -\left(\rho\omega^2/A_{11}\right)r^3 \tag{5}$$

where $()'$ refers to differentiation with respect to r. The complete solution of the preceding equation is in the following form:

$$u = C_1 r^{\lambda} + C_2 r^{-\lambda} + \frac{\rho\omega^2}{A_{11}(\lambda^2 - 9)} r^3 \tag{6}$$

where λ is defined as

$$\lambda = \sqrt{A_{22}/A_{11}}$$

Note that for $\lambda^2 = 9$, i.e., when the circumferential stiffness of the plate is nine times the radial stiffness, the solution according to Eq. (6) becomes unbounded. In this case, Eq. (5) is resolved to yield the following expression for radial displacement:

$$u = D_1 r^3 + D_2 r^{-3} + \frac{(1 - 6\ln r)}{36A_{11}}\rho\omega^2 r^2 \tag{7}$$

where unknown constants C_1, C_2 and D_1, D_2 are determined from the appropriate boundary conditions. For a full plate, the boundary conditions are $u(0) = 0$ and $u(R) = 0$. In this case, the second term in Eqs. (6) and (7) yields an infinite displacement at $r = 0$. For the displacement to be bounded, C_2 and D_2 must be zero, and the following expressions are obtained for C_1 and D_1:

$$C_1 = -\frac{\rho\omega^2 R^3}{R^{\lambda} A_{11}(\lambda^2 - 9)}, \qquad D_1 = -\frac{\rho\omega^2(1 - 6\ln R)}{36A_{11}} \tag{8}$$

Now that $u(r)$ is fully determined, the radial stress N_r is readily calculated from Eq. (3) as

$$N_r = \rho\omega^2 \frac{\left[(A_{12} + \lambda A_{11})r^{\lambda}R^3 - (A_{12} + 3A_{11})r^3 R^{\lambda}\right]}{A_{11}(9 - \lambda^2) r R^{\lambda}} \qquad (\lambda^2 \neq 9) \tag{9}$$

$$N_r = \rho\omega^2 \frac{[(A_{12} + 3A_{11})\ln(R/r) - A_{11}]r^2}{6A_{11}}, \qquad (\lambda^2 = 9) \tag{10}$$

If the plate is fixed to a rigid shaft of radius a, the boundary conditions are that there is no radial displacement at $r = a$ and R. The constants C_1, C_2 and D_1, D_2 are then expressed as

$$C_1 = -\frac{\rho\omega^2(R^{3+\lambda} - a^{3+\lambda})}{A_{11}(9 - \lambda^2)(R^{2\lambda} - a^{2\lambda})}$$
$$C_2 = -\frac{\rho\omega^2 R^{\lambda}a^{\lambda}(R^{\lambda}a^3 - R^3 a^{\lambda})}{A_{11}(9 - \lambda^2)(R^{2\lambda} - a^{2\lambda})} \tag{11}$$

$$D_1 = -\frac{\rho\omega^2\left[R^6(\ln R - 1/6) - a^6(\ln a - 1/6)\right]}{6A_{11}(R^6 - a^6)}$$
$$D_2 = -\frac{\rho\omega^2 R^2 a^6 \ln(a/R)}{6A_{11}(R^6 - a^6)} \tag{12}$$

and the corresponding radial stresses are

$$N_r = \frac{\rho\omega^2}{A_{11}(\lambda^2 - 9)(R^{2\lambda} - a^{2\lambda})} \times \left\{\left[a^{3+\lambda}(A_{12} + A_{11}\lambda)r^{2\lambda} + (A_{11}\lambda - A_{12})R^{2\lambda}\right] + a^{2\lambda}\left[(A_{12} - \lambda A_{11})R^{3+\lambda} - (A_{12} + 3A_{11})r^{3+\lambda}\right] + R^{2\lambda}r^{3+\lambda}\left[(A_{12} + 3A_{11}) - R^{3+\lambda}r^{2\lambda}(A_{12} + 3A_{11})\right]\right\} \qquad (\lambda^2 \neq 9) \tag{13}$$

$$N_r = \frac{\rho\omega^2(A_{12}/A_{11})}{6r^4(a^6 - R^6)}\left\{\left[a^6 r^6 \ln\frac{a}{r} + a^6 R^6 \ln\frac{R}{a} + R^6 r^6 \ln\frac{r}{R}\right] + \left[r^6(a^6 - R^6) + 3a^6 r^6 \ln\frac{r}{a} + 3R^6 a^6 \ln\frac{R}{a} + 3R^6 r^6 \ln\frac{R}{r}\right]\right\} \qquad (\lambda^2 = 9) \tag{14}$$

When the outer boundary is restrained from radial expansion, compressive radial stress is built up near the fixed edge. This stress buildup may be reduced by using laminates of stiffness ratio higher than one as shown by Tutuncu.[8] At high angular speeds, it is conceivable that these stresses might cause local stability problems. The next section will deal with determining the critical speed that will cause buckling.

III. Derivation of the Governing Equations of Stability

Consider a circular plate of radius R and uniform thickness h subjected to a compressive load $N_r(r)$ applied radially at the midplane of the plate. Figure 1 shows the plate geometry and forces and moments acting on a plate element. Because of the axisymmetry of the problem, all stresses and strain components are θ independent, and the force and moment equilibrium equations take the following form.[14]

1) Force equilibrium equation in z direction:

$$\frac{1}{r}\frac{\mathrm{d}}{\mathrm{d}r}\left[(rN_{rz}) - \left(rN_r\frac{\mathrm{d}w}{\mathrm{d}r}\right)\right] = 0 \tag{15}$$

2) Moment equilibrium in r direction:

$$\frac{1}{r}\left[\frac{\mathrm{d}}{\mathrm{d}r}(rM_r) - (M_\theta)\right] + N_{rz} = 0 \tag{16}$$

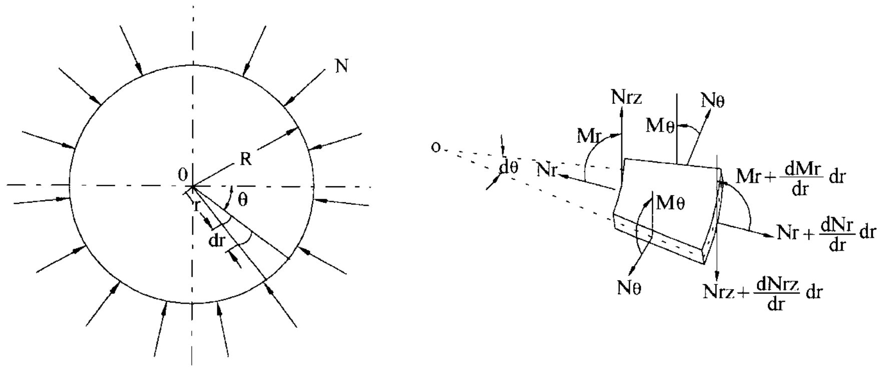

Fig. 1 In-plane forces and moments.

Here, w is the transverse displacement. Substituting N_{rz} from Eq. (16) into Eq. (15) yields

$$(1/r)[(rM_r)' - M_\theta] + rN_r w' = 0 \tag{17}$$

The curvature-transverse displacement relations are

$$\kappa_r = -w'', \qquad \kappa_\theta = -(1/r)w', \qquad \kappa_{r\theta} = 0 \tag{18}$$

The moment-curvature relationship may then be written for a specially orthotropic plate as

$$\begin{Bmatrix} M_r \\ M_\theta \\ M_{r\theta} \end{Bmatrix} = \begin{bmatrix} D_{11} & D_{12} & 0 \\ D_{21} & D_{22} & 0 \\ 0 & 0 & D_{66} \end{bmatrix} \begin{Bmatrix} \kappa_r \\ \kappa_\theta \\ 0 \end{Bmatrix} \tag{19}$$

where the bending stiffness terms are defined as follows[13]:

$$[D] = \frac{1}{3}\sum_{k=1}^{n}\left[Q^{(k)}\right]\left\{Z_{k+1}^3 - Z_k^3\right\}$$

With M_r and M_θ now defined in terms of D_{ij} and w, Eq. (17) may be written as

$$\{rw''' + w'' - [(1/r)(D_{22}/D_{11}) - r(N_r/D_{11})]w'\}' = 0 \tag{20}$$

The minimum N_r rendering a nonzero w is the buckling load. Because N_r is a function of the rotational speed in the present problem, the minimum ω satisfying the preceding equation will be called the critical speed. For a constant load $N_r = -N$, Eq. (20) can be solved in terms of Bessel functions.[15] However, when N_r is due to centrifugal forces, it assumes a complicated form, as Eqs. (9), (10), (13), and (14) indicate. Substituting either of these expressions for N_r in Eq. (20) will leave no choice but to resort to numerical methods.

IV. Weak Form of the Equation

In this section, our primary objectives will be to construct the weak form of Eq. (20) and to classify the boundary conditions associated with the equation. The weak form of the problems in solid mechanics can be developed either from the principle of virtual work or from the governing differential equation. We shall start with the given differential equation and use the three-step procedure to obtain the weak form for a full plate and a plate fixed to a rigid shaft. Rewrite Eq. (20) as, for $r1 < r < r2$,

$$\frac{\mathrm{d}}{\mathrm{d}r}\left[\frac{\mathrm{d}}{\mathrm{d}r}\left(-r\frac{\mathrm{d}^2 w}{\mathrm{d}r^2}\right) + \left(\frac{1}{r}\frac{D_{22}}{D_{11}} - r\frac{N_r}{D_{11}}\right)\frac{\mathrm{d}w}{\mathrm{d}r}\right] = 0 \tag{21}$$

A. Full Plate

Equation (21) may be integrated once. The resulting constant of integration is zero due to the continuity requirement on w at $r = 0$ (Ref. 9). Multiplying Eq. (21), after integrating once, by a weight function ψ and integrating over the whole domain gives us the weighted-residual statement equivalent to the original equation:

$$\int_{r1}^{r2} \psi\left\{\left[\frac{\mathrm{d}}{\mathrm{d}r}\left(-r\frac{\mathrm{d}^2 w}{\mathrm{d}r^2}\right) + \left(\frac{1}{r}\frac{D_{22}}{D_{11}} - r\frac{N_r}{D_{11}}\right)\frac{\mathrm{d}w}{\mathrm{d}r}\right]\right\}\mathrm{d}r = 0 \tag{22}$$

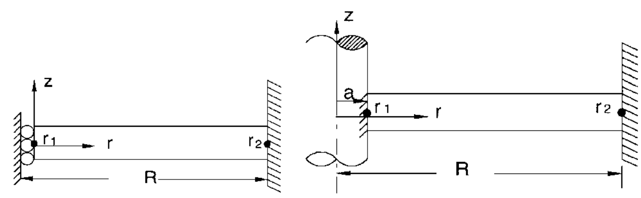

a) Full plate **b) Plate fixed to a rigid shaft**

Fig. 2 Problem model.

Integration of the first term by parts results in

$$\int_{r1}^{r2}\left\{\frac{\mathrm{d}\psi}{\mathrm{d}r}\left[\left(r\frac{\mathrm{d}^2 w}{\mathrm{d}r^2}\right) + \psi\left(\frac{1}{r}\frac{D_{22}}{D_{11}} - r\frac{N_r}{D_{11}}\right)\frac{\mathrm{d}w}{\mathrm{d}r}\right]\right\}\mathrm{d}r$$
$$-\left(\psi\frac{\mathrm{d}^2 w}{\mathrm{d}r^2}\right)_{r1}^{r2} = 0 \tag{23}$$

Assuming $\psi = \delta(\mathrm{d}w/\mathrm{d}r)$ and observing the boundary conditions (Fig. 2a) $\mathrm{d}^3 w/\mathrm{d}r^3 = (\mathrm{d}w/\mathrm{d}r)|_{r1=0} = 0$ and $w = (\mathrm{d}w/\mathrm{d}r)|_{r2=R} = 0$ at $r = r1$ and $r2$, Eq. (23) reduces to

$$\int_{r1}^{r2}\left\{\frac{\mathrm{d}\psi}{\mathrm{d}r}\left[\left(r\frac{\mathrm{d}^2 w}{\mathrm{d}r^2}\right) + \psi\left(\frac{1}{r}\frac{D_{22}}{D_{11}} - r\frac{N_r}{D_{11}}\right)\frac{\mathrm{d}w}{\mathrm{d}r}\right]\right\}\mathrm{d}r = 0 \tag{24}$$

which is the weak form of Eq. (21).

B. Plate Fixed to a Rigid Shaft

The weighted-residual statement equivalent to Eq. (21) is

$$\int_{r1}^{r2}\psi\left\{\frac{\mathrm{d}}{\mathrm{d}r}\left[\frac{\mathrm{d}}{\mathrm{d}r}\left(-r\frac{\mathrm{d}^2 w}{\mathrm{d}r^2}\right) + \left(\frac{1}{r}\frac{D_{22}}{D_{11}} - r\frac{N_r}{D_{11}}\right)\frac{\mathrm{d}w}{\mathrm{d}r}\right]\right\}\mathrm{d}r = 0 \tag{25}$$

Integration of Eq. (25) by parts results in

$$\int_{r1}^{r2}\left\{\frac{\mathrm{d}^2\psi}{\mathrm{d}r^2}\left[\left(r\frac{\mathrm{d}^2 w}{\mathrm{d}r^2}\right) + \frac{\mathrm{d}\psi}{\mathrm{d}r}\left(\frac{1}{r}\frac{D_{22}}{D_{11}} - r\frac{N_r}{D_{11}}\right)\frac{\mathrm{d}w}{\mathrm{d}r}\right]\right\}\mathrm{d}r$$
$$+\,\psi\left\{\left[\frac{\mathrm{d}}{\mathrm{d}r}\left(-r\frac{\mathrm{d}^2 w}{\mathrm{d}r^2}\right) + \left(\frac{1}{r}\frac{D_{22}}{D_{11}} - r\frac{N_r}{D_{11}}\right)\frac{\mathrm{d}w}{\mathrm{d}r}\right]\right\}\Bigg|_{r1}^{r2}$$
$$+\left(\frac{\mathrm{d}\psi}{\mathrm{d}r}\frac{\mathrm{d}^2 w}{\mathrm{d}r^2}\right)_{r1}^{r2} = 0 \tag{26}$$

Assuming $\psi = \delta w$ and observing the boundary conditions (Fig. 2b) $w = (\mathrm{d}w/\mathrm{d}r)|_{r1=a} = 0$ and $w = (\mathrm{d}w/\mathrm{d}r)|_{r2=R} = 0$ at $r = r1$ and $r2$, Eq. (26) reduces to

$$\int_{r1}^{r2}\left\{\frac{\mathrm{d}^2\psi}{\mathrm{d}r^2}\left[\left(r\frac{\mathrm{d}^2 w}{\mathrm{d}r^2}\right) + \frac{\mathrm{d}\psi}{\mathrm{d}r}\left(\frac{1}{r}\frac{D_{22}}{D_{11}} - r\frac{N_r}{D_{11}}\right)\frac{\mathrm{d}w}{\mathrm{d}r}\right]\right\}\mathrm{d}r = 0 \tag{27}$$

which is the weak form of Eq. (25). Equations (24) and (27) are identical as expected. In obtaining these equations, however, to comply with the boundary conditions of each problem, different kinematically admissible weight functions have been selected.

V. Interpolation Functions and the Finite Element Model

The interpolation functions are the standard cubic Hermite polynomials used in one-dimensional finite element analysis[16]:

$$N_1^e = 1 - 3[(r - r_1)/r_e]^2 + 2[(r - r_1)/r_e]^3$$

$$N_2^e = -(r - r_1)[1 - (r - r_1)/r_e]^2$$

$$N_3^e = 3[(r - r_1)/r_e]^2 - 2[(r - r_1)/r_e]^3$$

$$N_4^e = -(r - r_1)\{[(r - r_1)/r_e]^2 - (r - r_1)/r_e\}$$

We now list the following definitions:

$$w = [N]\{u\} = [P][A]^{-1}\{u\}$$

where $[N]$ is the matrix of interpolation functions; $[P] = [1, r, r^2, r^3]$ is the polynomial matrix; $[A]$ is the coefficient matrix, the inverse of which, when premultiplied by $[P]$, gives the matrix $[N]$; and the displacement vector $\{u\}$ is $\{w(r_1), -w'(r_1), w(r_2), -w'(r_2)\}$ (Fig. 3).

The finite element model of Eq. (24) is obtained by substituting the proper definitions of w and its derivatives in terms of interpolation functions along with the definition of ψ;

$$[\delta u]([A]^{-1})^T \int_{r1}^{r2} \left\{ r\{P\}''[P]'' + \frac{D_{22}}{D_{11}}\frac{1}{r}\{P\}'[P]' - r\frac{N_r}{D_{11}}\{P\}'[P]' \right\} \mathrm{d}r\, [A]^{-1}\{u\} = 0$$

Set the following definition (upon canceling out $[\delta u]$) and substitute N_r from Eqs. (10) and (11):

$$\sum_{j=1}^{n} \{[K_{ij}^e] - \omega^2[M_{ij}^e]\}[u_j^e] = 0 \qquad (28)$$

where $i = (1, 2, \ldots, n)$ is related to the number of elements and

$$[K_{ij}^e] = ([A]^{-1})^T[K_{ij}^*][A]^{-1}$$

where

$$[K_{ij}^*] = \int_{r1}^{r2} \left(\{P\}''[P]'' + \frac{D_{22}}{D_{11}}\frac{1}{r^2}\{P\}'[P]' \right) r\, \mathrm{d}r$$

Also,

$$[M_{ij}^e] = ([A]^{-1})^T[M_{ij}^*][A]^{-1}$$

where

$$[M_{ij}^*] = \int_{r1}^{r2} \left(\frac{r}{D_{11}}\{P\}'[P]' \right) \mathrm{d}r$$

Equation (28) represents an eigenvalue problem. The lowest value of ω is the critical rotational speed for the plate. The appropriate homogeneous boundary conditions are imposed by canceling the corresponding rows and columns in the assembled global system of equations.

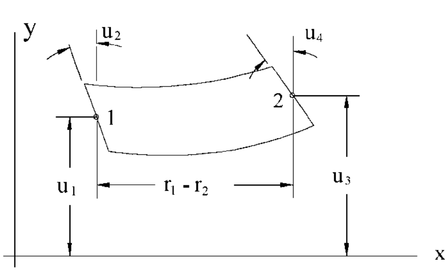

Fig. 3 Element with nodal displacement components.

VI. Results

For numerical work, 40-ply balanced laminates made from T300/5208 (graphite/epoxy) were used. The on-axis ($\Phi = 0$) elastic properties of a single ply are $Ex = 181$ GPa, $Ey = 10.3$ GPa, $Es = 7.17$ GPa, $\nu = 0.28$, and $t = 0.25 \times 10^{-4}$ m. The radius of the plate is $R = 0.5$ m for both the full plate and the plate fixed in its center to a rigid shaft of radius a. The accuracy of the present code has been tested on an isotropic full plate with elastic properties $\nu = \frac{1}{3}$, $E = 181$ GPa, and the same geometric properties. The exact critical speed for this case is calculated from the expression given in Ref. 9 as $\omega^*_{\text{isotropic}} = \omega\sqrt{\rho} = 343.279$. The present finite element code gives $\omega^*_{\text{isotropic}} = 344.355, 343.53$, and 343.289 when a radius is divided into 4, 8, and 20 elements, respectively. Because a good agreement with the exact result is achieved for 20 elements, the subsequent calculations for the composite plate are performed using the same number of elements. The normalized critical speed $\omega^*/\omega^*_{\text{isotropic}}$ for the composite plate is given in Fig. 4 as a function of the ply orientation Φ, for various a/R values. Note that the limiting case $a/R = 0$ corresponds to the full plate.

Figure 4 shows that the critical speed decreases up to about $\Phi = 55$ deg and starts to increase afterward. As for the plate fixed to a rigid shaft, the decrease in ω^* continues up to about $\Phi = 65$ deg with a slight increase afterward. As expected, increasing the radius of the rigid shaft increases the stability of the rotating plate. The highest critical speed is attained for $\Phi = 0$ deg. The stress distribution $N_r^* = N_r/\rho$ for $\Phi = 0$ deg at the critical speed is presented in Fig. 5 for the full plate and for the plate fixed to a rigid shaft for

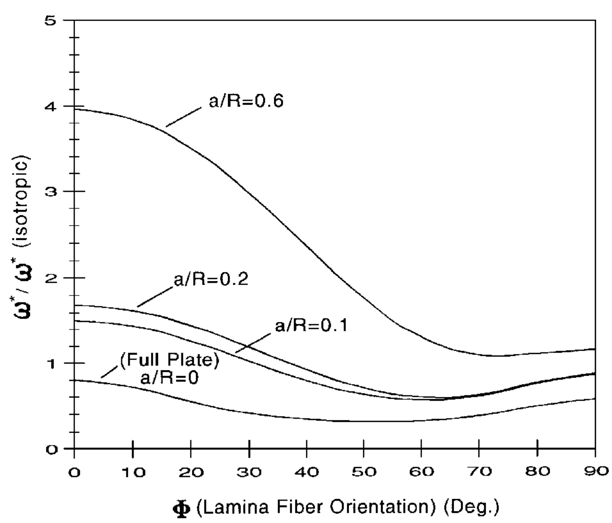

Fig. 4 Critical speed as a function of ply orientation angle for $(+\Phi, -\Phi)_{20}$ graphite/epoxy laminate.

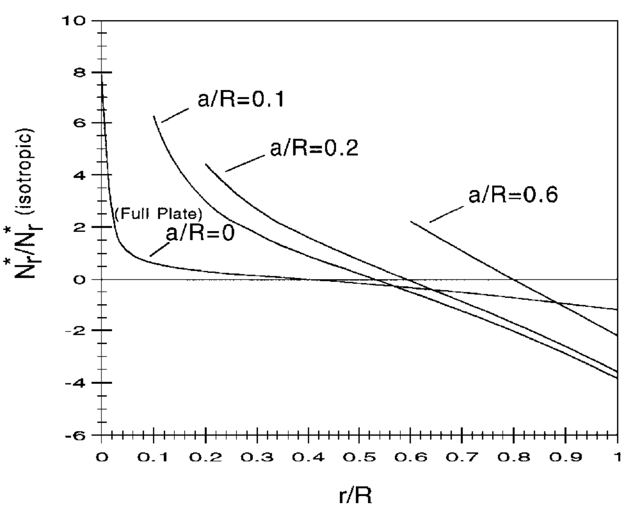

Fig. 5 Stress distribution at the critical speed as a function of ply orientation angle for $(+\Phi, -\Phi)_{20}$ graphite/epoxy laminate.

various a/R ratios. Stresses are normalized by $N_r^* = 4715$ Nm/kg, which is the maximum stress calculated at the critical speed $\omega^*_{\text{isotropic}}$ in the isotropic full plate at $r/R = 0$. The orthotropy contributes to a decrease in stability.

VII. Conclusions

Rotating orthotropic plates fixed along the outer boundary are subjected to compressive radial stresses near the fixed boundary. These stresses are functions of the distance from the center and of the ratio of the plate's circumferential stiffness to radial stiffness, which depend on the ply orientation angle. It is conceivable that at a certain critical angular speed the plate will buckle due to high compressive stresses.

In the present study, the critical speed for such plates is determined via a finite element formulation. It has been shown that increasing the orientation up to a certain point makes the plate less stable. In the case of a plate fixed to a rigid shaft, increasing the shaft radius causes the critical speed to increase, thereby increasing the stability of the plate.

References

[1]Reddy, T. Y., and Srinath, H., "Elastic Stresses in a Rotating Anisotropic Annular Disk of Variable Thickness and Variable Density," *International Journal of Mechanical Sciences*, Vol. 16, No. 2, 1973, pp. 85–89.

[2]Chang, C. I., "The Anisotropic Rotating Disks," *International Journal of Mechanical Sciences*, Vol. 17, No. 4, 1975, pp. 397–402.

[3]Gurushankar, G. V., "Thermal Stresses in a Rotating Nonhomogeneous Anisotropic Disk of Varying Thickness and Density," *Journal of Strain Analysis*, Vol. 10, No. 3, 1975, pp. 137–142.

[4]Christensen, R. M., and Wu, E. M., "Optimal Design of Anisotropic (fiber-reinforced) Flywheels," *Journal of Composite Materials*, Vol. 11, Oct. 1977, pp. 395–404.

[5]Genta, G., and Gola, M., "The Stress Distribution in Orthotropic Rotating Discs," *Journal of Applied Mechanics*, Vol. 48, Sept. 1981, pp. 559–562.

[6]Bert, C. W., "Centrifugal Stresses in Arbitrarily Laminated Rectangular-Anisotropic Circular Discs," *Journal of Strain Analysis*, Vol. 10, No. 2, 1975, pp. 84–92.

[7]Bert, C. W., and Niedenfuhr, F. W., "Stretching of a Polar-Orthotropic Disk of Varying Thickness Under Arbitrary Body Forces," *AIAA Journal*, Vol. 1, No. 6, 1963, pp. 1385–1390.

[8]Tutuncu, N., "Effect of Anisotropy on Stresses in Rotating Discs," *International Journal of Mechanical Sciences*, Vol. 37, No. 8, 1995, pp. 873–881.

[9]Mostaghel, N., and Tadjbakhsh, I., "Buckling of Rotating Rods and Plates," *International Journal of Mechanical Sciences*, Vol. 15, No. 6, 1973, pp. 429–434.

[10]Haughton, D. W., and Ogden, R. W., "Bifurcation of Rotating Circular Cylindrical Elastic Membranes," *Mathematical Proceedings of the Cambridge Philosophical Society*, Vol. 87, No. 4, 1980, pp. 357–376.

[11]Haughton, D. W., and Ogden, R. W., "Bifurcation of Rotating Thick-Walled Elastic Tubes," *Journal of the Mechanics and Physics of Solids*, Vol. 28, No. 1, 1980, pp. 59–74.

[12]Brunelle, E. J., "Stress Redistribution and Instability of Rotating Beams and Disks," *AIAA Journal*, Vol. 9, No. 4, 1971, pp. 758, 759.

[13]Tsai, S. W., and Hahn, H. T., *Introduction to Composite Materials*, Technomic, Lancaster, PA, 1980, Chap. 7.

[14]Timoshenko, S., and Woinowsky-Krieger, S., *Theory of Plates and Shells*, McGraw–Hill, New York, 1959, Chap. 3.

[15]Stavsky, Y., "Thermoelastic Stability of Laminated Orthotropic Circular Plates," *Acta Mechanica*, Vol. 22, No. 1, 1975, pp. 31–51.

[16]Shames, I. H., and Dym, C. L., *Energy and Finite Element Methods in Structural Mechanics*, Hemisphere, New York, 1985, Chap. 11.

G. A. Kardomateas
Associate Editor